Published in final edited form as:

Ann Surg. 2023 December 01; 278(6): e1289–e1298. doi:10.1097/SLA.0000000000005940.

Neutrophil and NETosis modulation in traumatic heterotopic ossification

Johanna H. Nunez, M.D.,
Department of Surgery, Center for Organogenesis and Trauma University of Texas, Southwestern, Dallas, TX

Conan Juan, B.S.,
Department of Surgery, Center for Organogenesis and Trauma University of Texas, Southwestern, Dallas, TX

Yuxiao Sun, Ph.D.,
Department of Surgery, Center for Organogenesis and Trauma University of Texas, Southwestern, Dallas, TX

Jonathan Hong, B.S.,
Department of Surgery, Center for Organogenesis and Trauma University of Texas, Southwestern, Dallas, TX

Alec C. Bancroft, B.S.A.,
Department of Surgery, Center for Organogenesis and Trauma University of Texas, Southwestern, Dallas, TX

Charles Hwang, M.D.,
Department of Plastic Surgery, Harvard University, Cambridge, MA

Jessica Medrano, M.S,
Department of Surgery, Center for Organogenesis and Trauma University of Texas, Southwestern, Dallas, TX

Amanda K. Huber, Ph.D.,
University of Michigan, Department of Radiation Oncology, Ann Arbor, MI

Robert J Tower, Ph.D.,
Department of Surgery, Center for Organogenesis and TraumaUniversity of Texas, Southwestern, Dallas, TX

Benjamin Levi, M.D.
Department of Surgery, Center for Organogenesis and Trauma University of Texas, Southwestern, Dallas, TX

Corresponding authors: **Benjamin Levi, MD,** Lee-Hudson Professor and Division Chief of General Surgery, Director, Center for Organogenesis and Trauma, University of Texas Southwestern Medical Center, Benjamin.Levi@UTSouthwestern.edu, **Robert Tower, PhD** Assistant Professor, Center for Organogenesis and Trauma, Charles and Jane Pak Center for Mineral Metabolism, University of Texas Southwestern Medical Center, Robert.Tower@UTSouthwestern.edu.

Conflict of Interest declaration: The authors declare that they have no affiliations with or involvement in any organization or entity with any financial interest in the subject matter or materials discussed in this manuscript.

Abstract

Objective: To characterize the role of neutrophil extracellular traps (NETs) in heterotopic ossification formation and progression and to use mechanical and pharmacological methods to decrease NETosis and mitigate heterotopic ossification (HO) formation.

Summary Background Data: Traumatic heterotopic ossification (HO) is the aberrant osteochondral differentiation of mesenchymal progenitor cells following traumatic injury, burns, or surgery. While the innate immune response has been shown to be necessary for HO formation, the specific immune cell phenotype and function remains unknown. Neutrophils, one of the earliest immune cells to respond following HO inducing injuries, can extrude DNA, forming highly inflammatory neutrophil extracellular traps. We hypothesized that neutrophils and NETs would be diagnostic biomarkers and therapeutic targets for the detection and mitigation of HO.

Methods: C57BL6J mice underwent burn/tenotomy (BT) (a well-established mouse model of HO) or a non-HO-forming sham injury. These mice were either 1) ambulated ad libitum, 2) ambulated ad libitum with daily intraperitoneal hydroxychloroquine (HCQ), ODN-2088 (both known to affect NETosis pathways), or control injections, or 3) had the injured hind limb immobilized. Single-cell analysis was performed to analyze neutrophils, NETosis, and downstream signaling following the HO-forming injury. Immunofluorescence (IF) microscopy was used to visualize NETosis at the HO site and neutrophils were identified using flow cytometry. Serum and cell lysates from HO sites were analyzed using ELISA for MPO-DNA and ELA2-DNA complexes to identify NETosis. Micro-CT (uCT) was performed on all groups to analyze the HO volume.

Results: Molecular and transcriptional analyses revealed the presence of NETs within the HO injury site, which peaked in the early phases after injury. These NETs were highly restricted to the HO site, with gene signatures derived from both in vitro NET induction and clinical neutrophil characterizations showing a high degree of NET “priming” at the site of injury, but not in neutrophils in the blood or bone marrow. Cell-cell communication analyses revealed that this localized NET formation coincided with high levels of Toll-like receptor (TLR) signaling specific to neutrophils at the injury site. Reducing the overall neutrophil abundance within the injury site, either pharmacologically through treatment with hydroxychloroquine (HCQ), the TLR9 inhibitor OPN-2088, or mechanical treatment with limb offloading, results in mitigation of HO formation.

Conclusions: These data provide a further understanding of the ability of neutrophils to form NETs at the injury site, clarify the role of neutrophils in HO, and identify potential diagnostic and therapeutic targets for HO mitigation.

Neutrophils, the earliest immune cells to respond following heterotopic ossification (HO) inducing injuries, can extrude DNA, forming highly inflammatory neutrophil extracellular traps (NETs). This study characterized the role of NETs in HO formation and progression and used mechanical immobilization and pharmacological methods to decrease NETosis and mitigate HO formation.

Keywords

Neutrophils; Neutrophil extracellular traps (NET); Heterotopic Ossification (HO); hydroxychloroquine; Toll-like Receptors (TLRs); ODN-2088

Introduction.

Heterotopic ossification (HO) is the pathological formation of extraskeletal bones. It can occur after musculoskeletal trauma and burns and is found in approximately 20% of patients following total hip arthroplasty and in 64% of patients with high-energy musculoskeletal injuries[1–3]. Neutrophil activity is one of the earliest immune responses to injury[4,5]. Once neutrophils reach the injury site, they extrude their DNA, creating neutrophil extracellular traps (NETs) via a process known as NETosis[6,7]. NETs comprise neutrophil DNA, histones, and degradation enzymes, such as myeloperoxidase (MPO) and neutrophil elastase (ELA2). The primary function of NETs is their antimicrobial properties[8]. However, neutrophils are also stimulated to release NETs after trauma[9] and in autoimmune disease flares such as rheumatoid arthritis and lupus[10,11].

Although HO is known to form after an inflammatory event, there are currently no early diagnostic biomarkers or therapeutic interventions that can effectively target neutrophil function. Standardized treatment for HO is lacking, and surgery fails to restore pre-injury functional capacity and is associated with a high risk of recurrence. Current prophylactic approaches (bisphosphonates, glucocorticoids, nonsteroidal anti-inflammatory therapeutics[12–17], and radiation therapy[18–24]) have had limited success, causing adverse effects and inconsistent outcomes. In addition to current non-specific therapies, the appropriate timing to initiate treatment and the treatment duration remain unknown. Once HO is diagnosed, physicians restrict movement of the affected joint to limit progression; however, the mechanism behind limiting mobility to alter inflammation and HO progression remains unknown. Thus, there is a substantial need to develop an effective biomarker to guide patient selection and precise therapeutic timing as well as inflammation-targeted HO therapies.

Here, we aimed to determine the diagnostic and regulatory roles of neutrophils and NETs in a previously characterized trauma-induced HO model of aberrant osteochondral cell differentiation[25]. During HO disease formation and progression, our data indicate that neutrophils represent a large population of cells at the HO site, and that these cells express high levels of transcripts associated with NET formation. Furthermore, we provide evidence that markers of NET formation may serve as early diagnostic markers for HO. Although neutrophils are also present in the bone marrow and blood, they are less prone to undergo NET formation. Given previous findings on the impact of mechanical stress causing the propagation of primary inflammation-driven NETosis during HO formation[4], we examined the effect of immobilization on systemic and local NETosis and showed evidence of decreased injury site NETosis. Next, we investigated the upregulated pathways in neutrophils following injury and found that TLR were highly upregulated at the site of musculoskeletal injury. Treatment with clinically relevant inhibitors of TLR signaling significantly decreased HO formation. In summary, neutrophils are early responders to extremity trauma and undergo NET formation at HO sites and can serve as diagnostic biomarkers and therapeutic targets to mitigate this debilitating process.

Methods:

Study Approval

All animal experiments were approved by the University of Texas Southwestern Dallas (2020–103004). All animal procedures were performed in accordance with the Guide for the Use and Care of Laboratory Animals: Eighth Edition of the Institute for Laboratory Animal Research.

Mouse Use and Treatments

The mice were housed under standard conditions. All animals were male (8–10 week old) C57BL/6 mice purchased from The Jackson Laboratory (000664). All treatment groups were cohoused with members of their treatment group for 1 week prior to surgery and following treatment until they were euthanized to ensure similar gut microbiomes. All the mice received preoperative slow-release SQ buprenorphine for analgesia. The animals were anesthetized by isoflurane inhalation. Mice that underwent burn/tenotomy (BT) were subjected to 30% total body surface area partial-thickness dorsal burns and Achilles tenotomy. Dorsal burns were induced using a metal block heated to 60°C in a water bath, which was then applied to the shaved mouse dorsum for 18 s. Tenotomy was performed via the transection of the left Achilles tendon. Animals were either assigned to mobilize ad libitum or to undergo BT with immediate hindlimb immobilization (as previously described)[26] following injury. The mice received daily intraperitoneal injections of hydroxychloroquine (60 mg/kg), ODN-2088 (0.00015 mg/kg), or sterile water (control). Treatment was administered on day 0 post-surgery. Mice were euthanized on days 1, 3, 7, 14, 21, and 63 after injury for analysis.

Single-cell RNA sequencing (scRNA-seq)

Seurat package v4 was used for filtering, uniform manifold approximation and projection (UMAP) dimensionality reduction analysis, and standard clustering of the 3-day post-injury marrow, blood, HO, 7-day post-injury mobilized (control) vs. immobilized, and 0-day, 7-day, and 42-day post-injury datasets. NET scores were calculated using the *AddModuleScore* function with induced NETosis genes obtained from *in vitro* RNA sequencing of neutrophils following NET induction with PMA/A23187[27] and pathologic NETosis genes obtained from patient neutrophils with a higher propensity for NET formation[28] (Supplementary Table 1). An overall NET score was calculated for the pathologic NETosis genes by subtracting the module score for downregulated genes from that of the upregulated genes.

Histology and Immunofluorescent Staining

Full-leg samples were harvested 3, 7, 14, 21, and 63 days after BT injury. Legs were fixed in 4% paraformaldehyde (PFA) for 24h at 4°C, washed three times with phosphate-buffered saline (PBS, Gibco, Waltham, MA), and decalcified using 17% ethylenediaminetetraacetic acid (EDTA, pH 7.4) for five weeks (Sigma Aldrich, St. Louis, MO, USA). Tissues were then embedded in optimal cutting temperature (OCT) media (Sakura, Torrance, CA, USA) to prepare sagittal sections of frozen tissues. Sections were cut at 12 μm for

immunofluorescence and at 5 μm for Safranin-O imaging on Fisher SuperFrost Microscopy slides (Fisher, Pittsburgh, PA, USA). For immunofluorescence staining, sections were thawed and washed in 1X tris-buffered saline with .05% tween-20 (TBS-T:1xTBS (Bio-Rad, Hercules, CA), tween-20 (Thermofisher, Waltham, MA)). Sections were blocked with donkey serum blocking solution (1% BSA, 2% donkey serum, 0.1% cold water fish skin gelatin, 0.05% TritonX-100, 0.05% Tween-20, 300mM glycine, 1x TBS,pH 8.4) for 2 h at room temperature (RT), and then incubated at 4°C overnight with primary antibodies (Ly6g: Abcam AF1062, 1:100; MPO: R&D AF3667, 1:100; Histone H3: Abcam ab5103, 1:100), washed in 1X TBS-T three times, and incubated with fluorescence-conjugated secondary antibodies for 2 h at RT (Invitrogen donkey anti-rat AF488, Invitrogen donkey anti-rabbit AF555, Invitrogen donkey anti-goat AF647, all secondary 1:200 dilution, Carlsbad, CA). The slides were then stained for nuclei with Hoechst 33342 (Thermo Fisher, Waltham, MA) for 5 min, washed in 1X TBS-T, and mounted with ProLong Glass Antifade Mountant (Invitrogen, Carlsbad, CA) and #1.5 Slip-Rite cover glass (Richard-Allan Scientific, San Diego, California). For immunofluorescence imaging of 10-micron murine sections, 1x and 1.58x computerized zoom images were captured using a 40x oil-immersion lens on a Leica Stellaris 8 confocal microscope.

Luminex Assay

Serum levels of mouse cytokines were measured using the Bio-Rad 23-plex Luminex immunoassay kit (#M60009RDPD) following the manufacturer's protocol. Data were collected using the MAGPIX® system (Luminex Corporation, Austin, TX, USA). To quantify individual factors, all standards were run in parallel and a corresponding standard curve was created. All data were within the linear portions of the curves. Assays were performed by UT Southwestern Genomics and Microarray Core Facility, and the technician was blinded to experimental conditions.

ELISA Analysis

Mice were treated, and serum and HO sites were harvested as described above for MPO and ELA2-DNA ELISAs. Capture antibodies were prepared by diluting mELA2 and MPO antibodies to the desired concentration (2–10ug/ml) in PBS without the carrier protein. 100ul were then added to each well to coat the plate overnight at 4°C. The coating solution was then removed from the wells and the plate was washed three times with 300ul PBS. The plate was blocked with 300ul of 5% BSA in PBS for 1–2 hours at room temperature. The samples were then added to the plate (4-fold or 2 to10-fold dilution in 5% BSA) with the plain sample diluent used in the blank plate. 0–3 ul of 100-fold diluted DNase (0.3 mg/ml) was added to each well, with a final concentration of DNase ranging from 0 to 0.9ug/ml reaction mixture. The plates were then incubated at room temperature for 15 min. 1ul 0.5M EDTA was added to each well to stop the DNase reaction and then was incubated overnight. Following incubation, the solution was thoroughly removed from the wells and the plate three times with 300ul PBST (0.05% Tween 20 in PBS). Diluted peroxidase-conjugated anti-DNA antibody was added at a ratio of 1:40 with 1% BSA in PBS (if not digested with DNase, 1 100 dilution) and incubated at room temperature for 90 min. After washing, 100uL TMB substrate solution was added to each well and incubated for 5–20 minutes until the

color appeared. The OD of each well was measured at 650 nm or 450 nm after adding 50ul 1M HCl / 2M H2SO4 stop solution.

OPLL Microarray Analysis

Microarray analyses of ossification of the posterior longitudinal ligament (OPLL) were performed using the NIH Gene Expression Omnibus (GSE5464). Cultured and cyclically strained cells derived from these ectopic ossifications were analyzed as previously described[29,30] between the ossified OPLL samples and non-ossifying controls (n=2/group). The expression profiles of all microarray genes and samples were extracted, normalized (log_2), and examined over the value distributions for quality control. The normalized expression values were fitted to a linear model using *limma*. All resulting entries without corresponding ENTREZ ID were excluded. The resulting matrix was sorted in descending order of the absolute values of all the expression values. Any duplicate gene symbols with smaller values were summarized, resulting in 1546 remaining genes. NETosis gene lists and associated pathways [27] were subsequently examined (induced NETosis, pathological NETosis, and TLR9 signaling). The heat maps demonstrate significant self-clustering between the control and the OPLL samples. NETosis scores were calculated by summing the expression values of each gene in each sample. Bar plots display the respective mean NETosis scores (with standard deviation), n=2/group.

Flow Cytometry:

Following a burn/tenotomy injury, at timepoints of 3 and 7 days the soft tissue from the posterior compartment between the muscular origin and the calcaneal insertion of the Achilles tendon was dissected out and collected for processing. The tissue was digested for 20–30 min in 0.3% type 1 collagenase and 0.4% Dispase II (Gibco) in Roswell Park Memorial Institute (RPMI) medium at 37°C under constant agitation at 180 rpm. The digestions were quenched with 10% FBS in RPMI and then filtered through 40μm sterile strainers. Samples were blocked with anti-mouse CD16/32 and subsequently stained with antibodies against Ly6G, CD11b, Ly6C, and CD45. Samples were washed with FACs buffer (2% FBS in PBS) and flow cytometry data were collected using a FACSCanto flow cytometer (BD Biosciences). The analysis was performed using the FlowJo software.

Micro-Computerized Tomography Imaging and Quantification

Micro-CT images were obtained at the University of Texas Southwestern using the Mediso USA Nano Scan PET/CT System (Arlington, VA, USA). The scanning parameters were a maximum zoom with 720 helical projections, X-ray power of 70 kV at 980 μA, and exposure time of 300ms. Scans were analyzed using the Dragonfly ORS by a blinded operator who manually scored ectopic bone at a single threshold of 800 Hounsfield units (HU). In addition to total ectopic bone, the results were further subdivided into “bone-associated” ectopic bone contiguous with the calcaneus, “floating” ectopic bone independent of the calcaneus, “proximal” ectopic proximal to the tenotomy site, and “distal” ectopic bone distal to the tenotomy site.

Statistical Analysis

GraphPad Prism 9 (San Diego, CA) was used to perform statistical testing. Normality and heterogeneity of variance tests were run to ensure appropriate statistical tests were used. Statistical significance is displayed on each graph as an asterisk (*) for unpaired two-tailed Student's *t* test. In experiments with multiple groups or treatments, statistical significance is displayed on each graph as an asterisk (*) for one-way analysis of variance test with Tukey's post-hoc test. Significance was set at $p< 0.05$. *$p < 0.05$, **$p < 0.01$, ***$p < 0.001$, and ****$p < 0.0001$.

Results

NETosis formation is stimulated by an HO inducing injury

Neutrophils are derived from the bone marrow, where they undergo progressive maturation before entering the blood and eventually reaching the site of injury. To determine the spatial specificity of neutrophil NETosis, we used our recently obtained scRNA-seq datasets (GSE221134) from cells at the HO site, blood, and bone marrow three days following burn/tenotomy (BT) injury. Single cells, represented by individual points, were clustered and identified based on similar gene expression using UMAP reduction (Fig. 1A, Supplemental Day 3 Cluster DEG), before being used for further analysis (Fig. 1B). Two NET gene scores were generated based on either *in vitro* RNA sequencing of neutrophils following NET induction with PMA/A23187 (denoted as induced NETosis)[27] or genetic signatures obtained from patient neutrophils with a higher propensity for NET formation (denoted as pathological NETosis)[28]. These module scores represent the average activation of their respective gene lists across each single cell, with higher module scores indicating higher average activation (red) and lower module scores indicating lower average activation (blue; Fig. 1C, Supp Figs. 1A–C). Genes from our induced NETosis gene list exhibited highly restrictive activation within the HO site (Fig. 1D), culminating in a higher induced NETosis score, with a larger percent of neutrophils (represented by larger dot size) showing higher average expression of this gene list (red), at the HO site (Fig. 1E), Similar results were observed when using the pathological gene list, which showed preferential gene activation within neutrophils present at the HO site (Supp Fig. 1C). To confirm HO site-specific activation of NET formation, we performed immunofluorescence analysis of the HO site. Previous studies have stained for MPO or H3Cit; however, the colocalization of these markers is necessary to establish a true NET. Therefore, we stained for MPO and H3Cit and observed a robust increase in NET formation at the HO sites following injury (Fig. 1F). Consistent with our histological findings, ELISAs for ELA2-DNA and MPO-DNA showed a significant increase in NET formation at the injury site after injury (Fig. 1G). Overall, these data suggest that NETs are robustly formed within HO sites after injury.

NETosis as an early marker to detect HO formation

Currently, early diagnosis is a major challenge for the care of patients with HO. While patients undergoing procedures at high risk for HO, such as hip replacement surgery, receive prophylaxis, such as radiation or NSAIDs, only some develop HO, leaving other patients exposed to the risk of these preventative interventions. Thus, we sought to determine whether early signs of NET formation could distinguish between HO- and non-HO-inducing

injuries. ELISAs were conducted on the tendon area of mice that had received HO-inducing BT injury or an inflammation-inducing dorsal burn plus skin incision over the Achilles tendon, which did not form HO (SI). Both ELA2-DNA (Fig. 2A) and MPO-DNA ELISAs (Fig. 2B) showed a significant increase in NETs following BT injury on days 7, 14, and 21 compared to SI controls. Our ELISA data suggested that NETs formed early after injury and persisted for several weeks.

To assess the impact of time after injury on NET signaling at the transcriptional level, we analyzed single-cell RNA sequencing data of neutrophils collected from the HO site prior to injury and at 7- and 42-days post-injury[31]. Using our NET scores for both induced (Fig. 2C–D) and pathologic NETosis (Fig. 2E), we found that NET signaling was dramatically higher 7 days post-injury than at later time points, suggesting that NET signaling in neutrophils peaks rapidly following injury.

Immobilization reduces NET formation and inflammatory cytokines

Immobilization has previously been shown to reduce HO formation[32] and is thought to reduce secondary NETosis by decreasing mechanical stress on the tissue[4]. To assess whether NETosis was affected in our model, we analyzed a previously published scRNA-seq of the HO site seven days post-BT (GSE150995)[32] (Fig. 3A) and showed that immobilization decreased both induced and pathological NETosis scores (Fig. 3B). To confirm these results, ELISAs for NET markers were conducted at the injury site in mice that were either uninjured or underwent BT surgery, with or without immobilization (Fig. 3C). These results show that while BT injury significantly increased the levels of ELA2-DNA and MPO-DNA compared to both SI and uninjured controls, BT with immobilization significantly reduced ELA2-DNA levels, with a trend towards reduced MPO-DNA ($p=0.057$) compared to BT alone. Consistent with our previous scRNA-seq analysis, only minimal levels of NETs were detected in serum after either injury (Supplementary Fig. 2).

In addition to reducing NET formation, we examined the effects of immobilization on cytokine production. Cytokines play an important role in inflammatory cascades. IL-6 has previously been shown to induce neutrophilia,[33]plays a crucial role in neutrophil trafficking[34], mobilization[35], and the transition from neutrophil to monocyte recruitment[36] and has recently been linked to NETosis in COVID patients[37]. On days 1, 3, 7, and 14 post injury, IL-6 levels were significantly higher following BT than in either uninjured or SI mice (Fig. 3D). The increased IL-6 levels were significantly reduced in mice that underwent BT surgery with immobilization (Fig. 3D). IL-1α, as previously shown, triggers neutrophil accumulation and NET production through IL-1R1 dependent pathways[38,39] and can elicit NET formation through NET-associated proteases that cleave IL-1α to its active form[39–41]. Similar to IL-6, IL-1α levels significantly increased in the BT group, which was mitigated in response to immobilization (Fig. 3E). These data suggest that immobilization results in reduced production of inflammatory cytokines and reduced production of NETs stimulated by HO-forming BT injury.

Upregulation of TLR and NETosis pathways in Ectopic Bone Formation

Our data suggest that, while inflammatory cascades are activated throughout the mouse by BT injury, NET-related gene expression and associated formation are restricted to the HO injury site. To further understand this area-specific regulation, we conducted cell-cell communication analyses on our scRNA-seq data obtained from the bone marrow, blood, and HO following BT, looking at the sequential activation of receptors by their ligands, their downstream transcription factors, and the transcription factor target genes (Fig. 4A). These analyses were used to identify downstream cellular signals activated within neutrophils as a result of ligand-receptor interactions occurring within each of the sequenced sites. Pathway analysis of these downstream targets within HO site neutrophils showed significant enrichment, indicated by higher -log(p-value), in several well-established inflammatory cascades, including Toll-like receptor (TLR) signaling, a pathway known to regulate NET formation (Fig. 4B)[42,43]. Although present to some extent within neutrophils across our three physiological sites, a comparison of TLR-related signaling within neutrophils revealed a substantial and significant enrichment in TLR signaling, specifically at the HO site (Fig. 4C).

To correlate these findings with human disease, we examined ossification of the posterior longitudinal ligament (OPLL), which is another form of ectopic bone formation that occurs in ligamentous tissue. Similar to HO formation in our mouse model, OPLL was examined because of mechanical stress/disruption of the tissue[29,44] leading to aberrant ossification. Using microarray data from human spinal ligament cells, NET and TLR9 pathways were investigated. When analyzed, the relative NET activity and TLR9 pathways in OPLL ossification were significantly upregulated compared with those in non-ossifying human controls (Fig. 4D). These data suggest that NET formation may be regulated by TLR signaling, specifically within the HO injury site and other areas of aberrant ossification.

Mechanical and Pharmacologic modulation of neutrophils mitigates HO

Next, we sought to determine the potential role of upstream signaling and NETs in HO progression. Previous studies have shown that HCQ treatment can alter TLR and Peptidyl arginine deaminase 4 (PAD4) signaling and mitigate NET-induced injury[45,46]. Given our finding that immobilization also leads to decreased NET formation (Fig. 3C), we explored the effects of HCQ treatment and immobilization on HO (Fig. 5A). Micro-CT analysis of HCQ treated with HCQ for 9 weeks showed a statistically significant decrease in HO formation compared with controls (Fig. 5B). Similar to our previously published results, immobilization significantly reduced HO formation (Fig. 5B). Although the combined 9-week course of HCQ and immobilization treatment reduced HO to a greater extent than immobilization alone, these differences were not statistically significant ($p=0.15$) most likely due to the very small HO volumes after immobilization. These findings suggest that HCQ alone, as well as HCQ in combination therapy with immobilization, is effective in reducing HO.

HCQ or immobilization treatments may affect HO progression by modulating TLR-mediated NET formation or changes in overall neutrophil numbers. To assess changes in the overall number of neutrophils within the injury site, we performed flow cytometry

(Fig. 5B). Analyses revealed that, while only a trend towards reduced neutrophil numbers was observed in HCQ-treated mice 3 days post-BT (Fig. S3), by day 7, a significant reduction was observed in the number of $CD45^+CD11B^+LY6G^+$ cells within the HO site of HCQ-treated or immobilized mice compared to that in BT-only controls, consistent with our previous work[4] (Fig. 5B).

To determine the role of TLR signaling and overcome the off-target effects of HCQ, we conducted additional BT studies on mice treated with the more specific TLR9 inhibitor ODN-2088 with drug treatment for a shorter two-week period (Fig. 5C). This TLR9 antagonist, which also has some additional inhibition of TLR 7/8, was chosen as TLR9 is a DNA sensing receptor known to be involved in some NETosis pathways[47]. Micro-CT analyses revealed that ODN-2088, similar to HCQ treatment, significantly mitigated bone-related and distal HO formation, and decreased overall HO formation (Fig. 5). We observed a similar decrease in HO formation when the mice were treated with HCQ for just two weeks compared to when they were treated with HCQ for nine weeks. Although HCQ is generally well tolerated, minimizing the treatment window is preferable because its long-term use can have adverse effects such as retinopathy and rarely cause cardiac and auditory toxicity[48]. These data suggest that modulation of NETs, either through changes in neutrophil numbers or inhibition of TLR9-mediated NET induction, can prevent HO formation.

Discussion:

Understanding neutrophil biology and how the neutrophil phenotype shifts from the bone marrow to the blood and eventually to the injury site is crucial for elucidating the immune response to injury. In this study, we characterized the migration, phenotype, and function of neutrophils and NETs after musculoskeletal injury. We discovered that neutrophils home to injured musculoskeletal tissue and undergo NET formation upon arrival at the injury site. Sequencing analyses suggested that this increased NETosis is associated with the upregulation of TLR signaling and that pharmacological inhibition of TLR9 signaling can mitigate HO formation, suggesting a potential new therapeutic strategy to prevent HO.

Our group and others previously examined the potential role of NET formation in extremity pathologies[4,45,49–51]. Importantly, these studies did not examine neutrophils from all the key compartments after injury (blood, bone marrow, and injury site). In our model of ectopic bone formation, we found through scRNA-seq that NETosis markers were not elevated in the bone marrow and blood after injury, and only became activated to undergo NET formation at the musculoskeletal injury site. Unlike previous studies of other diseases where NET levels in the blood serve as a biomarker for autoimmune diseases and a marker of COVID severity[10,11,37,52], our burn and tendon injuries were insufficient to induce a statistically significant level of difference in NETs in the blood using several of the most commonly used ELISAs for NET formation. These findings may be explained by the inhibitory effects of serum[53] or by the fact that neutrophils in the blood do not interact with other tissue-resident cells such as MPCs, which we have shown to stimulate TLR9[54].

NET formation at the musculoskeletal injury site starting on day 3 was evidenced through ELISAs and single-cell sequencing, and was significantly elevated in the aberrant repair

occurring in our HO model compared to the normal repair seen in the burn and skin incision injury by day 7. Thus, NET levels may serve as biomarkers for predicting the development of HO in patients. Although this is only found at the HO site and not in the serum, many surgeries in which HO is a risk factor have a surgical drain in place, allowing the surgeon to sample the injury site and test NET levels to predict HO formation. Being able to predict future HO formation would enable more precise treatment timing and would prevent unnecessary and potentially harmful prophylaxis in patients who will not develop HO.

Previously, we showed that *in vitro* mechanical disruption of NETs increased secondary NET formation, while *in vivo* studies showed decreased NETs and HO formation by decreasing mechanical stress through immobilization[4]. Using single-cell sequencing, we compared both pathological and induced NETosis gene markers in our control BT versus immobilized HO sites, and found that NETosis markers were significantly decreased in the immobilized mouse cohort. Given that NETosis was upregulated in our HO forming injury model and reduced with immobilization, an important question that remains to be further assessed is the upstream molecular mechanism by which the injury site activates neutrophil NET formation.

Using scRNA-seq receptor-ligand matching and microarray analysis, our experiments suggest that TLR signaling is one of the main pathways enriched at the mouse HO site and is upregulated in an in vitro human model of aberrant tendon ossification (OPLL). This is congruent with previous studies that have identified toll-like receptors, which are key receptors for DNA recognition[4,55,56], as potential regulators of neutrophil NET formation. Studies have also shown in vitro that hydroxychloroquine (HCQ) can decrease NET formation[57,58] with some studies showing mitigation of injury through inhibition of TLR by HCQ [45,59].

To mitigate NET formation, mechanical (limb immobilization) and pharmacological (HCQ) interventions were used. We found that 9 weeks of treatment with either HCQ or immobilization significantly decreased overall neutrophil number and HO formation. Observing the significant decrease in HO formation, we set out to decrease the duration of treatment (from 9 to 2 weeks) and test the more specific drug ODN-2088 (TLR 7/8/9 antagonist), which we have previously shown to decrease neutrophil infiltration[4]. These treatments resulted in the HCQ group still having a significant decrease in HO formation compared to the 9 weeks of treatment, whereas the mice treated with ODN-2088 showed a significant decrease in bone-associated and distal HO formation and tended towards a decrease in overall HO formation.

Although this study focused on neutrophils, we recognized that there were several additional inflammatory and noninflammatory cellular contributors to the HO niche that were not considered. The interaction of neutrophils with macrophages has not been specifically investigated, given our previous study on the macrophage phenotype in HO formation and progression[60]. Multiple studies by our group and others have shown that other immune cells, such as macrophages, B cells, and T lymphocytes, play a role in HO [61–63]. For instance, the requirement of myeloid cells in HO has been well-documented, including the central role of myeloid TGFB expression[60,64,65]. While we investigated TLR pathways in our study,

a recent study showed that hydroxychloroquine also works through the PAD4 pathway to inhibit NETosis[46]. Further investigations are needed to delineate the role of PAD4 in the inhibition of HO. Further studies are needed to determine the role and timing of mechanical or pharmacological interventions on other immune cell types at the site of injury.

In summary, we provide a comprehensive analysis of neutrophil and NET formation after extremity trauma in HO, and expand our understanding of how this process is regulated. Importantly, it is not currently known whether there is a threshold for NET levels required for HO formation, or whether there is a linear relationship between neutrophils, NETs, and HO. It is also possible that similar neutrophil-tissue interactions govern other acute and sub-acute bone injuries, such as fractures and osteoarthritis. With an improved understanding of these immune pathways and new molecular targets, we can enhance currently available therapeutic strategies to mitigate traumatic HO. Additional studies are necessary to elucidate the effect of neutrophils and immune cells on injury site repair and HO and whether specific inhibition of neutrophil phenotypes may prevent this pathology.

Supplementary Material

Refer to Web version on PubMed Central for supplementary material.

Acknowledgements:

We would like to thank S. Harris from the Department of Radiology at the University of Texas Southwestern for their assistance with uCT imaging. We would also like to thank the University of Texas Southwestern Microarray Core Facility for their assistance with Luminex assay processing and the University of Texas Southwestern Genomics core for their assistance in single-cell sequencing.

Funding Statement:

This study was supported by Grant *1R61 AR078072* from the National Institutes of Health.

Ethical Compliance:

All animal procedures were performed in accordance with the Guide for the Use and Care of Laboratory Animals: Eighth Edition of the Institute for Laboratory Animal Research. All procedures performed in this study involving human participants were in accordance with the ethical standards of the institutional and/or national research committee and the 1964 Helsinki Declaration and its later amendments or comparable ethical standards.

Data Access Statement:

Research data supporting this publication are available from the GEO Expression Omnibus repository (https://www.ncbi.nlm.nih.gov/geo/).

References

1. Davis TA, O'Brien FP, Anam K, Grijalva S, Potter BK, Elster EA. Heterotopic ossification in complex orthopaedic combat wounds: quantification and characterization of osteogenic precursor cell activity in traumatized muscle. The Journal of bone and joint surgery American volume. 2011;93(12):1122–1131. [PubMed: 21776549]
2. Potter BK, Burns TC, Lacap AP, Granville RR, Gajewski DA. Heterotopic ossification following traumatic and combat-related amputations. Prevalence, risk factors, and preliminary results of excision. The Journal of bone and joint surgery American volume. 2007;89(3):476–486. [PubMed: 17332095]

3. Ranganathan K, Loder S, Agarwal S, et al. Heterotopic Ossification: Basic-Science Principles and Clinical Correlates. J Bone Joint Surg Am. 2015;97(13):1101–1111. [PubMed: 26135077]
4. Agarwal S, Loder SJ, Cholok D, et al. Disruption of Neutrophil Extracellular Traps (NETs) Links Mechanical Strain to Post-traumatic Inflammation. Front Immunol. 2019;10:2148. [PubMed: 31708911]
5. S Scola M; Nycz D; Gallagher K; McCauley LK; Xu J; James AW; Agarwal S; Kunkel S; Mishina Y; Levi B SMHAHCCWMRLJVKPCPNLSVNNYL. Regulation of heterotopic ossification through local inflammatory monocytes in a mouse model of aberrant wound healing. Nature communications. 2019;In Press.
6. Brinkmann V, Laube B, Abu Abed U, Goosmann C, Zychlinsky A. Neutrophil extracellular traps: how to generate and visualize them. Journal of visualized experiments : JoVE. 2010(36).
7. Brinkmann V, Reichard U, Goosmann C, et al. Neutrophil extracellular traps kill bacteria. Science. 2004;303(5663):1532–1535. [PubMed: 15001782]
8. Kaplan MJ, Radic M. Neutrophil extracellular traps: double-edged swords of innate immunity. J Immunol. 2012;189(6):2689–2695. [PubMed: 22956760]
9. Martinod K, Witsch T, Farley K, Gallant M, Remold-O'Donnell E, Wagner DD. Neutrophil elastase-deficient mice form neutrophil extracellular traps in an experimental model of deep vein thrombosis. Journal of thrombosis and haemostasis : JTH. 2016;14(3):551–558. [PubMed: 26712312]
10. Chapman EA, Lyon M, Simpson D, et al. Caught in a Trap? Proteomic Analysis of Neutrophil Extracellular Traps in Rheumatoid Arthritis and Systemic Lupus Erythematosus. Front Immunol. 2019;10:423. [PubMed: 30915077]
11. Chen W, Wang Q, Ke Y, Lin J. Neutrophil Function in an Inflammatory Milieu of Rheumatoid Arthritis. J Immunol Res. 2018;2018:8549329.
12. Burd TA, Lowry KJ, Anglen JO. Indomethacin compared with localized irradiation for the prevention of heterotopic ossification following surgical treatment of acetabular fractures. The Journal of bone and joint surgery American volume. 2001;83-A(12):1783–1788. [PubMed: 11741055]
13. Fransen M, Neal B. Non-steroidal anti-inflammatory drugs for preventing heterotopic bone formation after hip arthroplasty. The Cochrane database of systematic reviews. 2004(3):CD001160.
14. Matta JM, Siebenrock KA. Does indomethacin reduce heterotopic bone formation after operations for acetabular fractures? A prospective randomised study. The Journal of bone and joint surgery British volume. 1997;79(6):959–963. [PubMed: 9393912]
15. Moore KD, Goss K, Anglen JO. Indomethacin versus radiation therapy for prophylaxis against heterotopic ossification in acetabular fractures: a randomised, prospective study. The Journal of bone and joint surgery British volume. 1998;80(2):259–263. [PubMed: 9546456]
16. Pakos EE, Ioannidis JP. Radiotherapy vs. nonsteroidal anti-inflammatory drugs for the prevention of heterotopic ossification after major hip procedures: a meta-analysis of randomized trials. International journal of radiation oncology, biology, physics. 2004;60(3):888–895. [PubMed: 15465207]
17. Karunakar MA, Sen A, Bosse MJ, Sims SH, Goulet JA, Kellam JF. Indometacin as prophylaxis for heterotopic ossification after the operative treatment of fractures of the acetabulum. The Journal of bone and joint surgery British volume. 2006;88(12):1613–1617. [PubMed: 17159174]
18. Coventry MB, Scanlon PW. The use of radiation to discourage ectopic bone. A nine-year study in surgery about the hip. The Journal of bone and joint surgery American volume. 1981;63(2):201–208. [PubMed: 6780568]
19. Gregoritch SJ, Chadha M, Pelligrini VD, Rubin P, Kantorowitz DA. Randomized trial comparing preoperative versus postoperative irradiation for prevention of heterotopic ossification following prosthetic total hip replacement: preliminary results. International journal of radiation oncology, biology, physics. 1994;30(1):55–62. [PubMed: 8083129]
20. Koelbl O, Seufert J, Pohl F, et al. Preoperative irradiation for prevention of heterotopic ossification following prosthetic total hip replacement results of a prospective study in 462 hips. Strahlentherapie und Onkologie : Organ der Deutschen Rontgengesellschaft [et al]. 2003;179(11):767–773.

21. Pellegrini VD Jr., Konski AA, Gastel JA, Rubin P, Evarts CM. Prevention of heterotopic ossification with irradiation after total hip arthroplasty. Radiation therapy with a single dose of eight hundred centigray administered to a limited field. The Journal of bone and joint surgery American volume. 1992;74(2):186–200. [PubMed: 1541613]
22. Seegenschmiedt MH, Goldmann AR, Martus P, Wolfel R, Hohmann D, Sauer R. Prophylactic radiation therapy for prevention of heterotopic ossification after hip arthroplasty: results in 141 high-risk hips. Radiology. 1993;188(1):257–264. [PubMed: 8511308]
23. Seegenschmiedt MH, Goldmann AR, Wolfel R, Hohmann D, Beck H, Sauer R. Prevention of heterotopic ossification (HO) after total hip replacement: randomized high versus low dose radiotherapy. Radiother Oncol. 1993;26(3):271–274. [PubMed: 8316658]
24. Hamid N, Ashraf N, Bosse MJ, et al. Radiation therapy for heterotopic ossification prophylaxis acutely after elbow trauma: a prospective randomized study. The Journal of bone and joint surgery American volume. 2010;92(11):2032–2038. [PubMed: 20810853]
25. Peterson JR, Agarwal S, Brownley RC, et al. Direct Mouse Trauma/Burn Model of Heterotopic Ossification. J Vis Exp. 2015(102):e52880.
26. Khan MA, Sahani N, Neville KA, et al. Nonsurgically induced disuse muscle atrophy and neuromuscular dysfunction upregulates alpha7 acetylcholine receptors. Can J Physiol Pharmacol. 2014;92(1):1–8. [PubMed: 24383867]
27. Petretto A, Bruschi M, Pratesi F, et al. Neutrophil extracellular traps (NET) induced by different stimuli: A comparative proteomic analysis. PLoS One. 2019;14(7):e0218946.
28. Chen N, He D, Cui J. A Neutrophil Extracellular Traps Signature Predicts the Clinical Outcomes and Immunotherapy Response in Head and Neck Squamous Cell Carcinoma. Front Mol Biosci. 2022;9:833771.
29. Iwasawa T, Iwasaki K, Sawada T, et al. Pathophysiological role of endothelin in ectopic ossification of human spinal ligaments induced by mechanical stress. Calcif Tissue Int. 2006;79(6):422–430. [PubMed: 17160579]
30. Lee S, Hwang C, Marini S, et al. NGF-TrkA signaling dictates neural ingrowth and aberrant osteochondral differentiation after soft tissue trauma. Nat Commun. 2021;12(1):4939. [PubMed: 34400627]
31. Pagani CA, Huber AK, Hwang C, et al. Novel lineage-tracing system to identify site-specific ectopic bone precursor cells. Stem Cell Reports. 2021.
32. Huber AK, Patel N, Pagani CA, et al. Immobilization after injury alters extracellular matrix and stem cell fate. J Clin Invest. 2020;130(10):5444–5460. [PubMed: 32673290]
33. Hashizume M, Higuchi Y, Uchiyama Y, Mihara M. IL-6 plays an essential role in neutrophilia under inflammation. Cytokine. 2011;54(1):92–99. [PubMed: 21292497]
34. Fielding CA, McLoughlin RM, McLeod L, et al. IL-6 regulates neutrophil trafficking during acute inflammation via STAT3. J Immunol. 2008;181(3):2189–2195. [PubMed: 18641358]
35. Florentin J, Zhao J, Tai Y-Y, et al. Interleukin-6 mediates neutrophil mobilization from bone marrow in pulmonary hypertension. Cellular & Molecular Immunology. 2021;18(2):374–384. [PubMed: 33420357]
36. Kaplanski G, Marin V, Montero-Julian F, Mantovani A, Farnarier C. IL-6: a regulator of the transition from neutrophil to monocyte recruitment during inflammation. Trends in Immunology. 2003;24(1):25–29. [PubMed: 12495721]
37. Mukhopadhyay S, Sinha S, Mohapatra SK. Analysis of transcriptomic data sets supports the role of IL-6 in NETosis and immunothrombosis in severe COVID-19. BMC Genom Data. 2021;22(1):49. [PubMed: 34775962]
38. Westerterp M, Fotakis P, Ouimet M, et al. Cholesterol Efflux Pathways Suppress Inflammasome Activation, NETosis, and Atherogenesis. Circulation. 2018;138(9):898–912. [PubMed: 29588315]
39. Pyrillou K, Burzynski LC, Clarke MCH. Alternative Pathways of IL-1 Activation, and Its Role in Health and Disease. Front Immunol. 2020;11:613170.
40. Clancy DM, Henry CM, Sullivan GP, Martin SJ. Neutrophil extracellular traps can serve as platforms for processing and activation of IL-1 family cytokines. Febs j. 2017;284(11):1712–1725. [PubMed: 28374518]

41. Folco EJ, Mawson TL, Vromman A, et al. Neutrophil Extracellular Traps Induce Endothelial Cell Activation and Tissue Factor Production Through Interleukin-1α and Cathepsin G. Arterioscler Thromb Vasc Biol. 2018;38(8):1901–1912. [PubMed: 29976772]
42. Wei WC, Liaw CC, Tsai KC, et al. Targeting spike protein-induced TLR/NET axis by COVID-19 therapeutic NRICM102 ameliorates pulmonary embolism and fibrosis. Pharmacol Res. 2022;184:106424.
43. Al-Khafaji AB, Tohme S, Yazdani HO, Miller D, Huang H, Tsung A. Superoxide induces Neutrophil Extracellular Trap Formation in a TLR-4 and NOX-dependent mechanism. Mol Med. 2016;22:621–631. [PubMed: 27453505]
44. Lee S, Hwang C, Marini S, et al. NGF-TrkA signaling dictates neural ingrowth and aberrant osteochondral differentiation after soft tissue trauma. Nature Communications. 2021;12(1):4939.
45. Edwards NJ, Hwang C, Marini S, et al. The role of neutrophil extracellular traps and TLR signaling in skeletal muscle ischemia reperfusion injury. FASEB journal : official publication of the Federation of American Societies for Experimental Biology. 2020;34(12):15753–15770. [PubMed: 33089917]
46. Ivey AD, Fagan BM, Murthy P, et al. Chloroquine reduces neutrophil extracellular trap (NET) formation through inhibition of peptidyl arginine deiminase 4 (PAD4). Clin Exp Immunol. 2023.
47. Chen T, Li Y, Sun R, et al. Receptor-Mediated NETosis on Neutrophils. Front Immunol. 2021;12:775267.
48. Misra DP, Gasparyan AY, Zimba O. Benefits and adverse effects of hydroxychloroquine, methotrexate and colchicine: searching for repurposable drug candidates. Rheumatol Int. 2020;40(11):1741–1751. [PubMed: 32880032]
49. Navratilova A, Becvar V, Baloun J, et al. S100A11 (calgizzarin) is released via NETosis in rheumatoid arthritis (RA) and stimulates IL-6 and TNF secretion by neutrophils. Scientific reports. 2021;11(1):6063. [PubMed: 33727634]
50. Schauer C, Janko C, Munoz LE, et al. Aggregated neutrophil extracellular traps limit inflammation by degrading cytokines and chemokines. Nature medicine. 2014;20(5):511–517.
51. Suzuki K, Tsuchiya M, Yoshida S, et al. Tissue accumulation of neutrophil extracellular traps mediates muscle hyperalgesia in a mouse model. Scientific reports. 2022;12(1):4136. [PubMed: 35264677]
52. Zuo Y, Yalavarthi S, Shi H, et al. Neutrophil extracellular traps in COVID-19. JCI Insight. 2020;5(11).
53. Neubert E, Senger-Sander SN, Manzke VS, et al. Serum and Serum Albumin Inhibit in vitro Formation of Neutrophil Extracellular Traps (NETs). Front Immunol. 2019;10:12. [PubMed: 30733715]
54. Jiang W, Xu J. Immune modulation by mesenchymal stem cells. Cell Prolif. 2020;53(1):e12712.
55. Kumagai Y, Takeuchi O, Akira S. TLR9 as a key receptor for the recognition of DNA. Adv Drug Deliv Rev. 2008;60(7):795–804. [PubMed: 18262306]
56. Müller T, Hamm S, Bauer S. TLR9-mediated recognition of DNA. Handb Exp Pharmacol. 2008(183):51–70. [PubMed: 18071654]
57. Guo Y, Gao F, Wang X, et al. Spontaneous formation of neutrophil extracellular traps is associated with autophagy. Sci Rep. 2021;11(1):24005.
58. Frangou E, Chrysanthopoulou A, Mitsios A, et al. REDD1/autophagy pathway promotes thromboinflammation and fibrosis in human systemic lupus erythematosus (SLE) through NETs decorated with tissue factor (TF) and interleukin-17A (IL-17A). Ann Rheum Dis. 2019;78(2):238–248. [PubMed: 30563869]
59. Zheng H, Zhang Y, He J, et al. Hydroxychloroquine Inhibits Macrophage Activation and Attenuates Renal Fibrosis After Ischemia-Reperfusion Injury. Front Immunol. 2021;12:645100.
60. Sorkin M, Huber AK, Hwang C, et al. Regulation of heterotopic ossification by monocytes in a mouse model of aberrant wound healing. Nature communications. 2020;11(1):722.
61. Ranganathan K, Agarwal S, Cholok D, et al. The role of the adaptive immune system in burn-induced heterotopic ossification and mesenchymal cell osteogenic differentiation. The Journal of surgical research. 2016;206(1):53–61. [PubMed: 27916375]

62. Kan L, Liu Y, McGuire TL, et al. Dysregulation of local stem/progenitor cells as a common cellular mechanism for heterotopic ossification. Stem cells. 2009;27(1):150–156. [PubMed: 18832590]

63. Torossian F, Guerton B, Anginot A, et al. Macrophage-derived oncostatin M contributes to human and mouse neurogenic heterotopic ossifications. JCI Insight. 2017;2(21).

64. Wang X, Li F, Xie L, et al. Inhibition of overactive TGF-beta attenuates progression of heterotopic ossification in mice. Nature communications. 2018;9(1):551.

65. Wang X, Xie L, Crane J, et al. Aberrant TGF-beta activation in bone tendon insertion induces enthesopathy-like disease. The Journal of clinical investigation. 2018;128(2):846–860. [PubMed: 29355842]

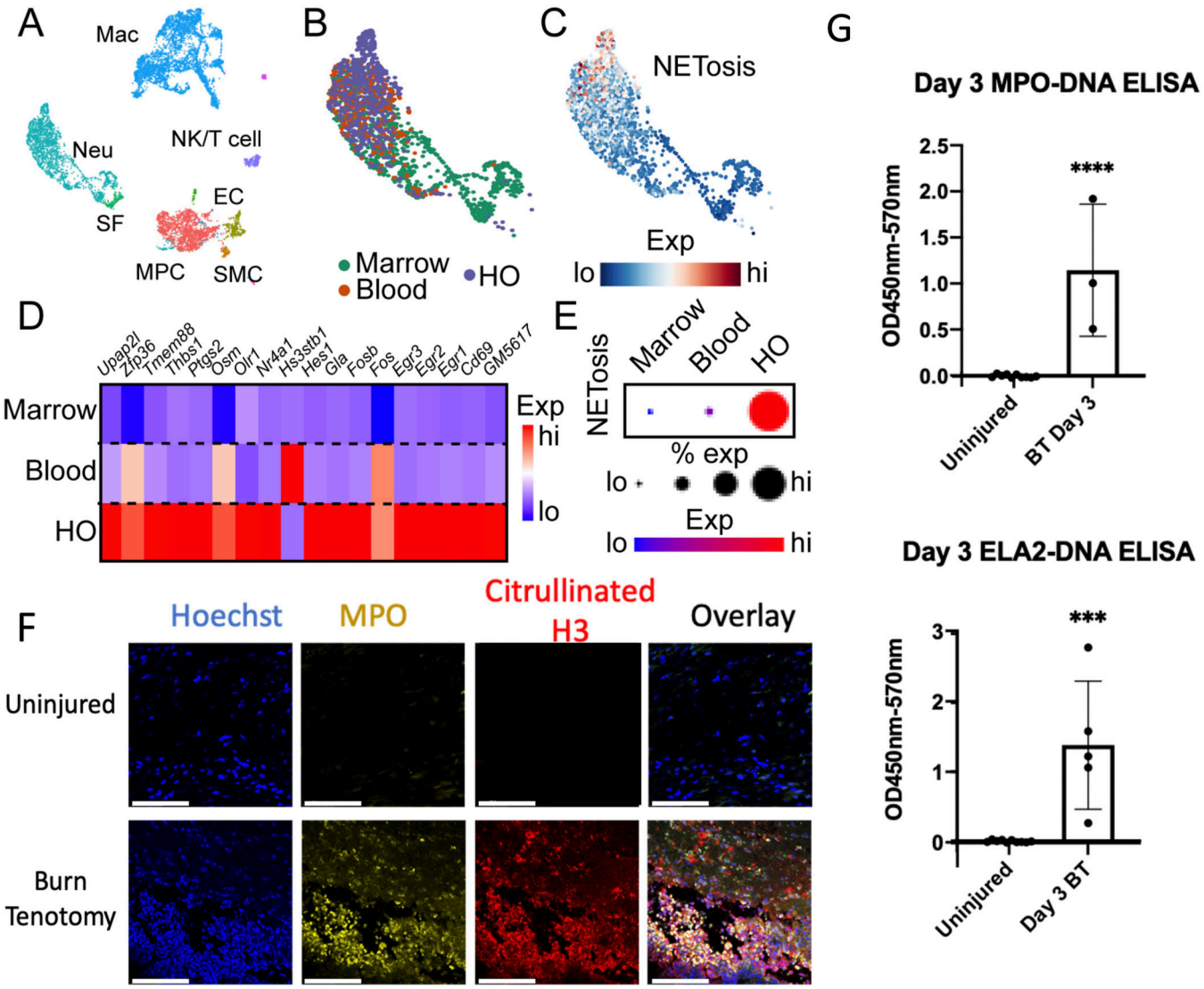

Figure 1. NET formation is stimulated by HO inducing injuries.

(A) UMAP plot of single cell RNA sequencing from cells harvested from the injury site (HO), blood, and tibial bone marrow 3 days post-BT injury, identifying multiple clusters. Single cells are represented by individual points. (B) UMAP plot of neutrophils colored by anatomical origin. (C) Feature plot of neutrophil expression of induced NETosis genes. Neutrophils with higher average expression of induced NETosis genes are red. (D) Heatmap showing average expression of individual genes upregulated in induced NETosis in neutrophils split by anatomical location. (E) Dot plot of overall expression of induced NETosis genes in neutrophils split by anatomical location. Dot size indicates percent of neutrophils expressing induced NETosis genes. Color indicates degree of expression, with red being high. (F) Immunofluorescent microscopy of the HO site at day 3 post-injury in an uninjured and burn/tenotomy. (G) Quantification of injury site MPO and ELA2 ELISAs in uninjured mice (n=10) as compared mice who underwent a burn/tenotomy (n=3/5). Scale bar represents 100 μm. (*** indicates $p < 0.001$, **** $p < 0.0001$).

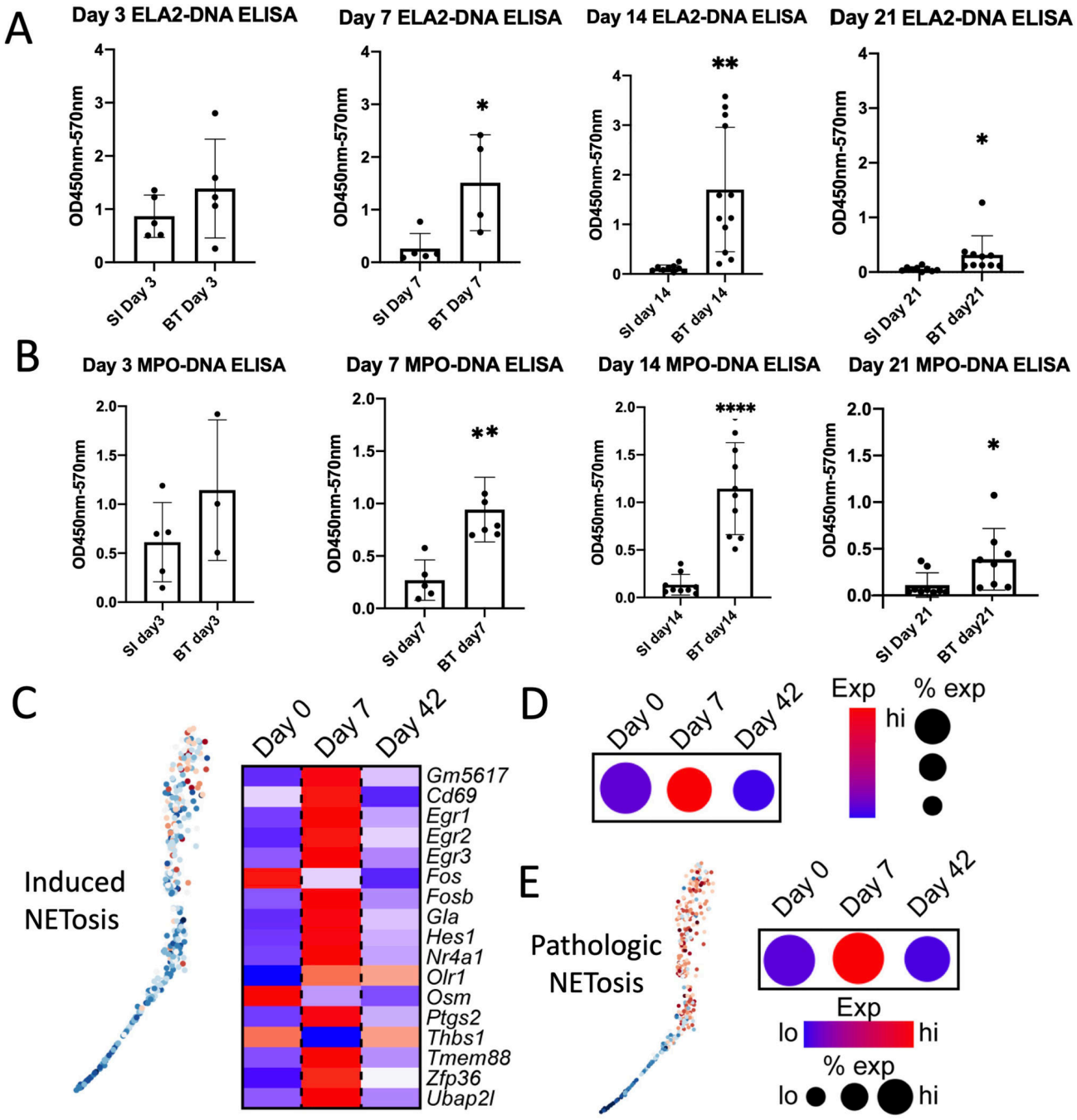

Figure 2. NETosis analysis to detect early HO formation.

Quantification of (A) ELA2-DNA ELISAs and (B) MPO-DNA ELISA done on cell lysate of the injury site following a non-HO forming burn and skin incision or a HO inducing burn/tenotomy injury at days 3, 7,14 and 21 (n=3–6/group). (C) Feature plot (left) and heatmap (right) of neutrophils harvested from the HO injury site of mice 0 days, 7 days, and 42 days post-BT injury showing expression of induced NETosis genes. Neutrophils with higher average expression of induced NETosis genes are red (left). (D) Dot plot of overall expression of induced NETosis genes in neutrophils split by timepoint. Dot

size indicates percent of neutrophils expressing induced NETosis genes. Color indicates degree of expression, with red being high. (E) Feature plot (left) and dot plot (right) of neutrophils harvested from the HO injury site of mice 0 days, 7 days, and 42 days post-BT injury showing expression of pathologic NETosis genes. Neutrophils with higher average expression of pathologic NETosis genes are red (left). Dot size indicates percent of neutrophils expressing pathologic NETosis genes. Color indicates degree of expression, with red being high (right). (* = $p<0.05$, ** = $p<0.01$, ****$p<0.001$). Stars indicate a significant increase as compared to the non-HO forming burn and skin incision.

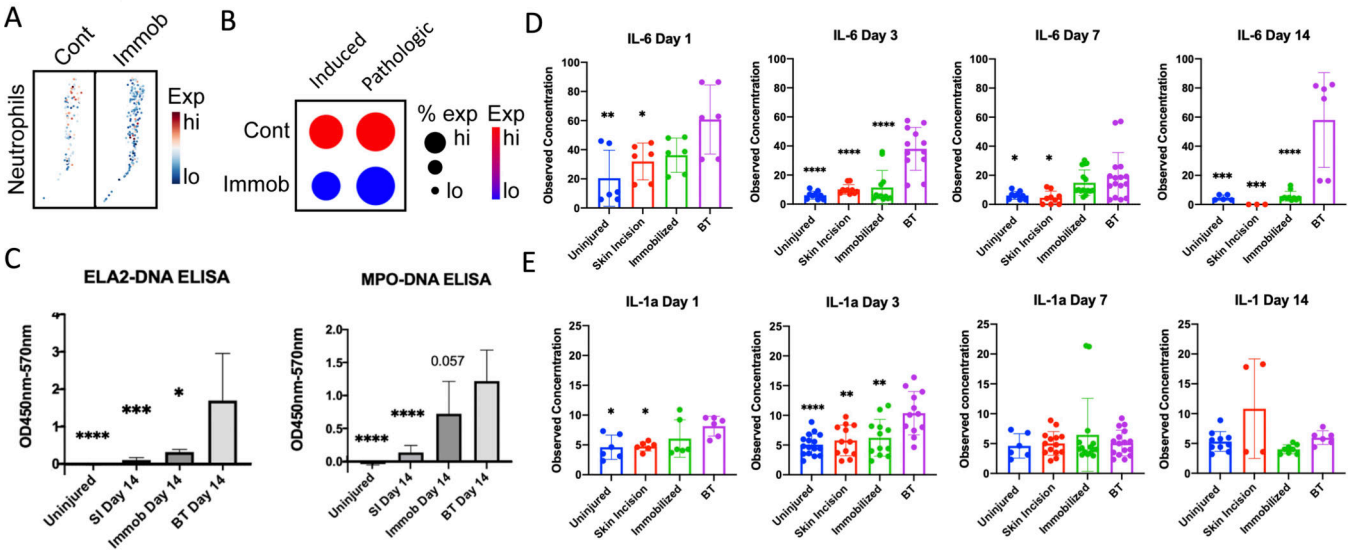

Figure 3. Immobilization effect on Injury Site NETosis and Serum Cytokines.

(A) Feature plot of neutrophils harvested from the HO injury site of mice 7 days post-BT injury from mobilized (control) and immobilized conditions, displaying expression of induced NETosis genes. Neutrophils with higher average expression of induced NETosis genes are red. (B) Dot plot of neutrophil expression of induced NETosis genes and net expression of pathologic NETosis genes. Dot size indicates percent of neutrophils expressing NETosis genes. Color indicates degree of expression, with red being high. (C) Quantification of ELA2-DNA ELISAs and MPO-DNA ELISAs done on day 14 cell lysate of the injury site following no injury, non-HO forming burn and skin incision (SI), HO inducing BT injury or HO inducing BT with post-injury hindlimb immobilization. (D) Quantification of mouse serum IL-1α and (E) IL-6 at days 1, 3, 7, and 14 following no injury, non-HO forming burn and (SI), HO inducing BT injury or HO inducing BT with post-injury hindlimb immobilization. * = $p<0.05$, ** = $p<0.01$, ***$p<0.001$, ****$p<0.0001$. Stars indicate a significant decrease as compared to the BT.

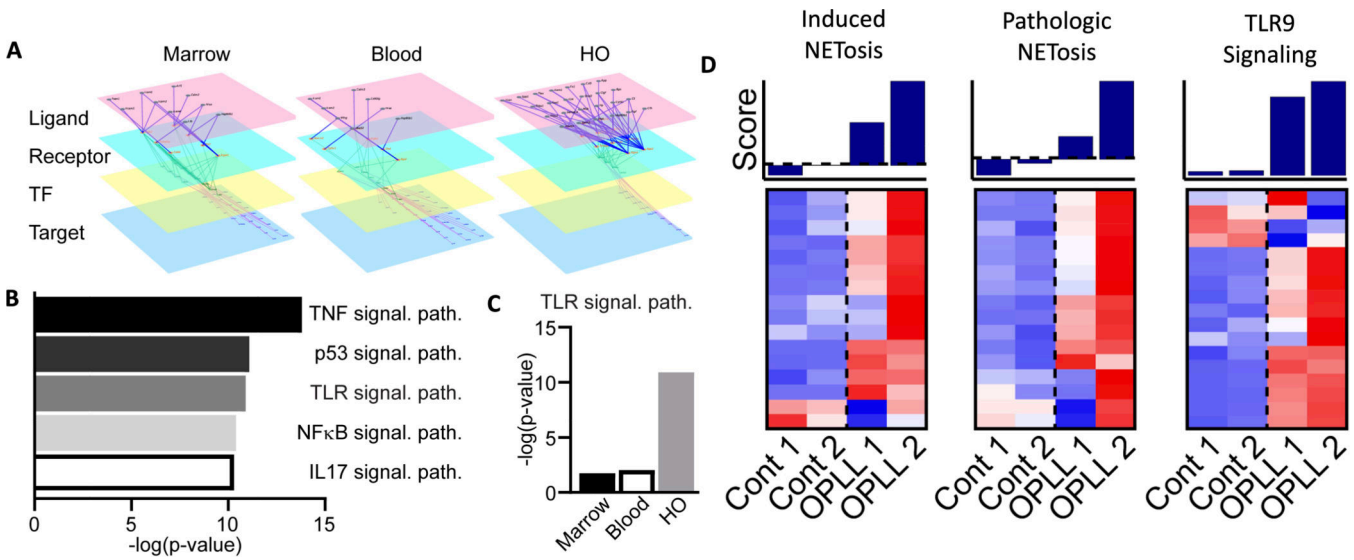

Figure 4. Upregulation of TLR and NETosis pathways in ectopic bone formation in a mouse and human model.

(A) Representative diagram of scRNA-seq based multilayer networks done by integrating intercellular pathways (ligand-receptor interactions) and intracellular subnetworks (receptor-transcription factor and transcription factor-target gene interactions) in relation to the neutrophil target. Sequential activation of receptors by their ligands, their downstream transcription factors, and the transcription factor target genes is shown. (B) Pathways upregulated in neutrophils at the HO injury site from scRNA-seq based multilayer network analysis. Higher -log(p-value) is associated with more enrichment of the pathway. (C) Inferred TLR9 pathway activation across anatomical sites. Higher-log(p-value) is associated with more enrichment of the pathway. (D) Microarray analyses of ossification of the posterior longitudinal ligament (OPLL) using gene lists for induced NETosis and pathologic NETosis, and TLR9 signaling pathways were compared in healthy controls (n=2) versus those with OPLL (n=2).

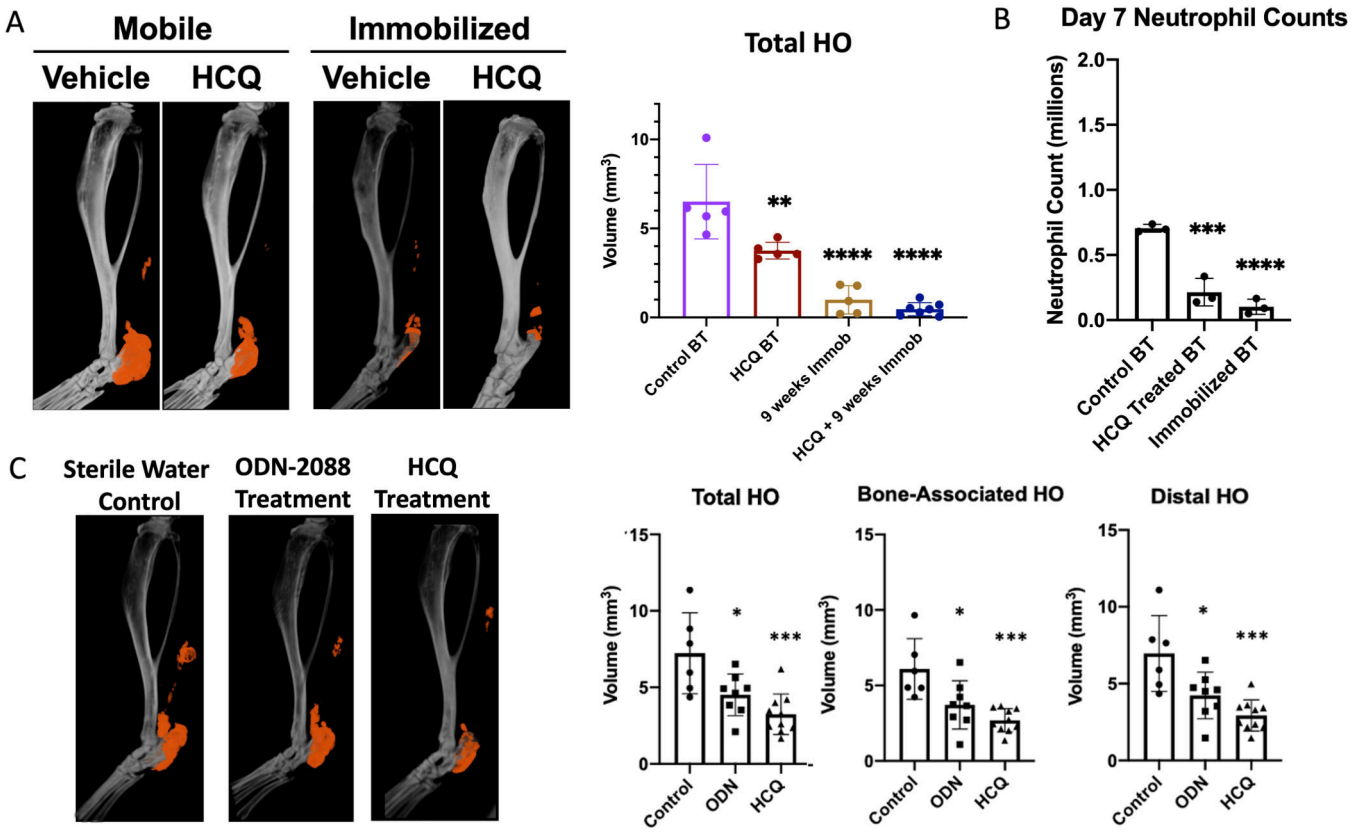

Figure 5. Mechanical and pharmacologic modulation of neutrophils mitigates HO.

(A) MicroCT analysis of tenotomy site 9 weeks after burn/tenotomy in mobilized versus immobilized mice following daily treatment of either sterile water (control) or hydroxychloroquine (HCQ). n=5–7/group. (B) Quantification of neutrophils ($CD45^+CD11b^+Ly6G^+$ cells) as assessed by flow cytometry at Day 7 post-injury in control BT, HCQ treated BT, and immobilized BT groups. n=3–4. (C) MicroCT analysis of tenotomy site 9 weeks after burn/tenotomy following 2 weeks daily injection of sterile water (control), ODN-2088 or HCQ. n=6–9. (* = $p<0.05$, ** = $p<0.01$, ****$p<0.001$). Stars indicate a significant decrease as compared to the control BT.